

# Excellence in Chemistry Research

## Announcing our new flagship journal

- Gold Open Access
- Publishing charges waived
- Preprints welcome
- Edited by active scientists



## Meet the Editors of *ChemistryEurope*



**Luisa De Cola**

Università degli Studi  
di Milano Statale, Italy



**Ive Hermans**

University of  
Wisconsin-Madison, USA

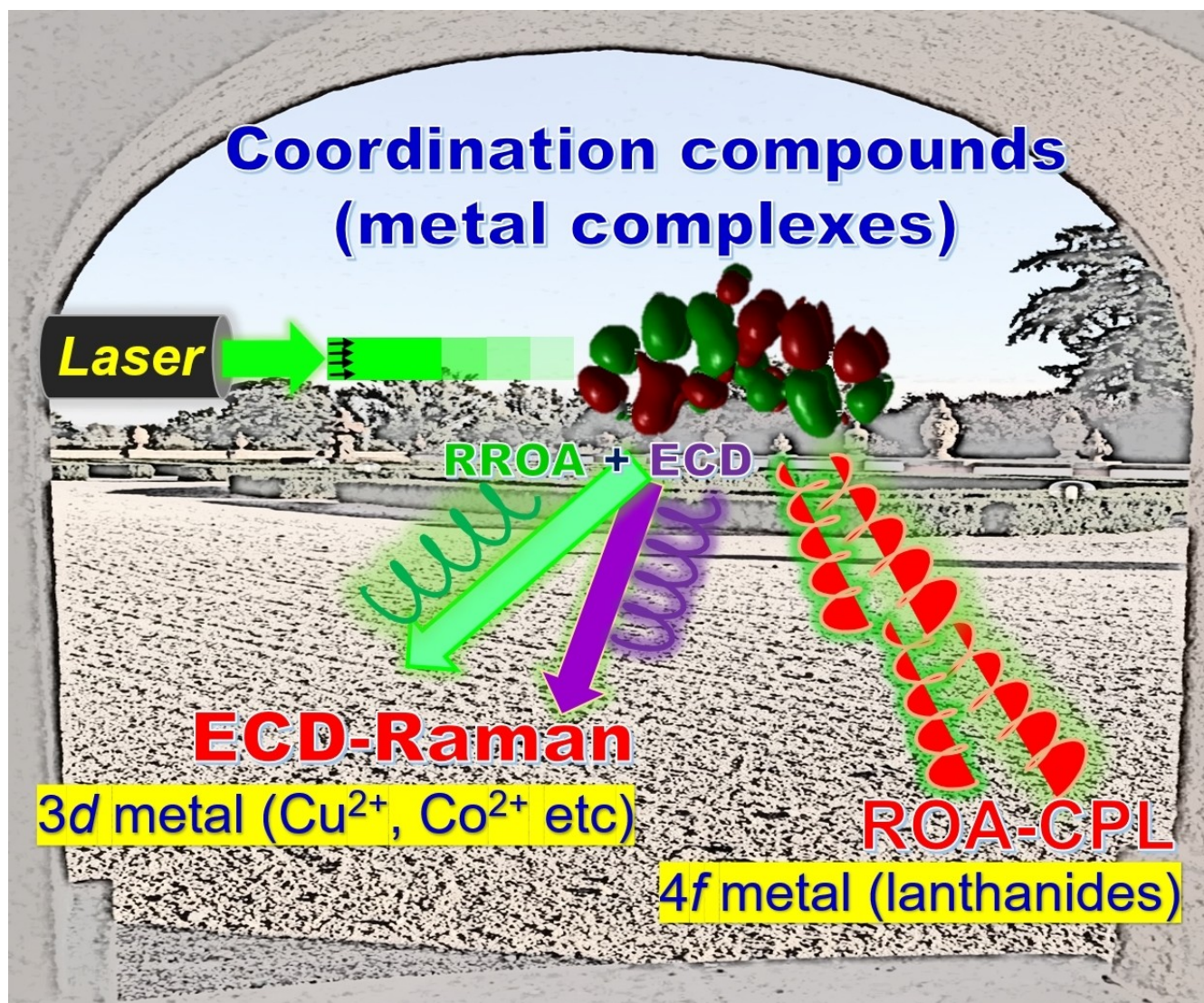


**Ken Tanaka**

Tokyo Institute of  
Technology, Japan

# Molecular Properties of 3d and 4f Coordination Compounds Deciphered by Raman Optical Activity Spectroscopy

Tao Wu,<sup>\*,[a]</sup> Radek Pelc,<sup>[a]</sup> and Petr Bour<sup>†[a]</sup>



Molecular properties of coordination compounds can be efficiently studied by vibrational spectroscopy. The scope of Raman spectroscopy has been greatly enhanced by the introduction of Raman optical activity (ROA) sensitive to chirality. The present review describes some of its recent applications to study the coordination compounds. 3d and 4f metal complexes often absorb the excitation light, or exhibit luminescence. Therefore, effects caused in ROA spectra by electronic circular dichroism (ECD) and circularly polarized luminescence (CPL) must be taken into consideration. In 3d metal complexes ECD and circularly-polarized Raman scattering

compete with the resonance ROA (RROA) signal. Pure RROA spectrum can thus be obtained by subtracting the so-called ECD-Raman component. CPL is frequently encountered in 4f systems. While it can mask the ROA spectra, it is useful to study molecular structure. These electronic effects can be reduced by using near-infrared excitation although vibrational ROA signal is much weaker compared to the usual green laser excitation scenario. The ROA methodology is thus complex, but capable of providing unique information about the molecules of interests and their interaction with light.

## 1. Introduction

Chirality is an intrinsic property of life as it is essential for the functioning of living organisms. Indeed, only L-forms of amino acids and D-forms of sugars can be utilized by them. Metalloproteins (alcohol dehydrogenases, cytochromes, myoglobin, vitamin B<sub>12</sub> etc) are no exception in this respect. In snails, chirality can be detected in the architecture of very early embryos consisting of only eight cells,<sup>[1]</sup> and is preserved to adulthood in the handedness of their shell.<sup>[1b,2]</sup> Chiral molecules are also essential in catalysis and materials science. The subject of studying the interaction of light with chiral molecules is the brainchild of Louis Pasteur.<sup>[3]</sup>

Coordination compounds with metal ions find numerous applications in industrial chemistry, materials and biological sciences.<sup>[4]</sup> Their structure and properties can be easily modified by molecular-chemistry tools, and studied in detail by molecular spectroscopy.

Chiroptical spectroscopy is capable of discerning differences in the interaction of left- and right-circularly polarized light with chiral molecules, and is frequently applied to chiral coordination compounds.<sup>[5]</sup> Most often, spectroscopic methods employed to detect chirality of coordination compounds involve electronic transitions in the ultraviolet and visible regions. Both electronic circular dichroism (ECD) sensitive to the stereochemistry of the ground state, and circularly polarized luminescence (CPL) suitable to examine excited states are used.

New possibilities emerged in the 1970s, when vibrational spectroscopy was coupled to optical activity measurements.<sup>[6]</sup> Vibrational circular dichroism (VCD) recording the optical activity in the infrared region is the vibrational analogue of ECD, whereas Raman optical activity (ROA) does not have an electronic counterpart.

Vibrational spectra generally contain a greater number of finely resolved bands when compared to electronic spectra.<sup>[6b]</sup> VCD has been commonly used in structural analyses of biomacromolecules, such as proteins and nucleic acids,<sup>[7]</sup> and more recently also to study metal complexes.<sup>[5a,c,10]</sup>

On the other hand, Raman spectroscopy is less commonly used to study coordination compounds,<sup>[9]</sup> and ROA spectroscopy is even rarer as the signal is very weak, thus requiring dedicated instrumentation.<sup>[5a,c,10]</sup> Moreover, coordination compounds with transitions in the visible spectral region are generally problematic for ROA typically fitted with a green (532 nm) laser. Obtaining a reliable ROA spectrum of molecular species absorbing the excitation light can be difficult because of sample fluorescence or decomposition.

Early applications of ROA spectroscopy to study the coordination compounds were accompanied by computational approaches although the development of proper theory was rather slow.<sup>[10b]</sup>

Nowadays, coordination compounds are studied by ROA more often. Owing to a better understanding of the role of electronic phenomena (ECD, CPL) in ROA spectra, extended information can be obtained. For example, 3d and 4f metal ions yield a strong ECD/ROA<sup>[11]</sup> and CPL/ROA<sup>[12]</sup> signal, respectively. The present review aims to describe such cases.

## 2. 3d Metal Coordination Compounds

It is a well-known fact that compared to Rayleigh scattering, Raman scattering is inherently very weak. Only when the photon energy matches an electronic energy level difference of the scattering sample a stronger (resonance) Raman signal may be generated. Its dependence on the excitation wavelength provides information about electronic energies, transition dipoles, molecular potential energy surfaces, etc. Resonance Raman spectroscopy is thus popular in inorganic chemistry.<sup>[13]</sup>

The resonance can also boost the ROA signal<sup>[14]</sup> and thus the circular intensity difference,<sup>[15]</sup>  $CID = (I_R - I_L)/(I_R + I_L)$  where  $I_R$  and  $I_L$  are the detected intensities of the right and left circularly polarized light. In resonance, the ROA signal is often even more enhanced than Raman, and the CID value (typically  $\sim 10^{-4}$  off-resonance) increases by an order of magnitude.<sup>[16]</sup> In this way, the vibrational chirality "borrows" its strength from the

[a] Dr. T. Wu, Dr. R. Pelc, Prof. P. Bouř  
Institute of Organic Chemistry and Biochemistry  
Czech Academy of Sciences  
Flemingovo náměstí 2  
16610 Prague (Czech Republic)  
E-mail: tao.wu@uochb.cas.cz

© 2023 The Authors. ChemPlusChem published by Wiley-VCH GmbH. This is an open access article under the terms of the Creative Commons Attribution Non-Commercial NoDerivs License, which permits use and distribution in any medium, provided the original work is properly cited, the use is non-commercial and no modifications or adaptations are made.

electronic one, such as that linked to the transition magnetic and electric moments of the resonant transition.

Resonance ROA (RROA) spectra involving both single<sup>[17]</sup> and more electronic states have been reported.<sup>[5c,14,18]</sup> In single state resonance ROA, the sign (of spectra) is often dependent on ECD at the excitation wavelength. The *CID* ratio is then related to the Kuhn's dissymmetry factor, i.e., the ratio of ECD and absorption spectra.<sup>[16b]</sup>

For most 3*d* metal coordination compounds, *d-d*, charge transfer or ligand-centered electronic transitions are detectable in ECD spectra.<sup>[5f,19]</sup> The transitions are categorized in a localized orbital model as ligand-to-metal, metal-to-ligand, ligand-to-ligand, or metal-to-metal charge-transfer. The simplified single electronic state model is sometimes appropriate, but it is generally not suitable for theoretical interpretation of more complex experimental RROA spectra.<sup>[16b]</sup>

The discovery of interference of ROA and ECD signals<sup>[11b]</sup> represents an important milestone in the development of the resonance ROA technique. Both circular dichroism and polarized Raman scattering have been shown to contribute to the observed "ROA" signal,  $I_R - I_L$ .<sup>[11a,20]</sup> This effect was designated as ECD-Raman.<sup>[16b]</sup> The measured signal of  $I_R - I_L$  is thus a sum of ECD-Raman and "true" RROA, as frequently encountered in 3*d* metal coordination compounds featuring transitions generating intense ECD signal in the visible region.<sup>[5f]</sup> The ECD-Raman effect is particularly intriguing in RROA measurements of achiral solvents, where strong ROA bands of the solvent may be encountered in the spectra. Initially, this phenomenon was incorrectly attributed to the complexation or intermolecular interactions between the achiral solvent(s) and a chiral solute.<sup>[21]</sup> Later, an accurate description of clear separation of RROA and ECD-Raman signals has been demonstrated.<sup>[11b,22]</sup> For *CID* due to ECD-Raman, we obtained

$$CID = \frac{I_R - I_L}{I_R + I_L} = \frac{\Delta\epsilon' + DOC\Delta\epsilon}{4} cl \quad (1)$$

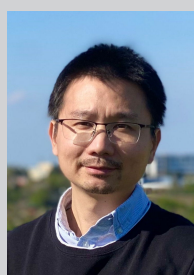
where  $\Delta\epsilon$  and  $\Delta\epsilon'$  are differential absorption coefficients (as relevant to ECD) of the excitation and scattered light, respectively; *c* is the concentration; *l* is the optical path length, and *DOC* is the degree of circularity of each vibrational transition of the solvent.<sup>[15]</sup>

Validity of this formula was demonstrated, for example, in a copper-porphyrin complex (CuOEP), using a double-cell magnetic circular dichroism (MCD) and magnetic ROA (MROA) experiments. The induced MROA signal of the solvent alone (i.e., control reference measurement) was recorded in the cell devoid of the chromophore complex ("solvent I" in Figure 1).<sup>[11b]</sup>

For the CuOEP complex, not only the induced ROA signal of chloroform (CHCl<sub>3</sub> as "solvent II" in Figure 1) could be observed, but also two bands attributed to the deuterated solvent (CDCl<sub>3</sub> as "solvent I" in Figure 1) that was not in contact with the dye. The MCD spectra of CuOEP<sup>[11b]</sup> indicate that dichroism of scattered light is much stronger compared to the incident one ( $|\Delta\epsilon'| > |\Delta\epsilon|$ ). This is consistent with the single-sign induced ROA bands below 900 cm<sup>-1</sup>.

In a most recent study,<sup>[11a]</sup> an improved ECD-Raman formula has been introduced, and Raman and ROA intensities could be corrected for auto-absorption with two 3*d* metal coordination compounds (Figure 2): (*R*, *R*)-(–)-N,N'-Bis(3,5-di-*tert*-butylsalicylidene)-1,2-cyclohexanediaminocobalt(II) (*R*-BuCo) and a tetrametallic copper(II) complex (*R*-Cubane). This methodology makes it easier to obtain more accurate RROA spectra.

The origin of the differential signal is a bit complicated, and is outlined for a Co(II) coordination compound in Figure 3. Raw ROA spectra, or more precisely the measured differences of  $I_R - I_L$ , exhibit quite different patterns for toluene and dichlorome-



Tao Wu is a scientist at the Institute of Organic Chemistry and Biochemistry of the Czech Academy of Sciences. He received his PhD in Chemistry from Nanjing University, China. He then undertook postdoctoral training in Nanjing and Prague. His research experience includes Saga University, Japan, which he joined as a senior visiting scholar supported by the European Union Social Fund. His research focus includes molecular chirality and chiroptical spectroscopy, lanthanide optical activity, and applications in biophysical chemistry and microscopic chemical imaging.



Radek Pelc received his DPhil in Physiology and Biophysics from Oxford University. His thesis on intracellular calcium signalling also included studies of transmembrane calcium fluxes at the BioCurrents Research Center of the Marine Biological Laboratory (Woods Hole, MA, USA). He then investigated the structure of myosin S1 molecular motor at Hamburg Synchrotron Laboratory DESY. Now he specializes in label-free imaging including Raman microscopy, and teaches microscopy techniques to medical students at Charles University.



Petr Bouř received his PhD from Czechoslovak Academy of Sciences. His postdoctoral training included University of Illinois at Chicago, University of Calgary, University of Tromsø, and University of Wyoming. His research focuses on spectral modeling and development of related computational approaches. He is a group leader at the Institute of Organic Chemistry and Biochemistry, and a professor at the University of Chemistry and Technology, Prague.

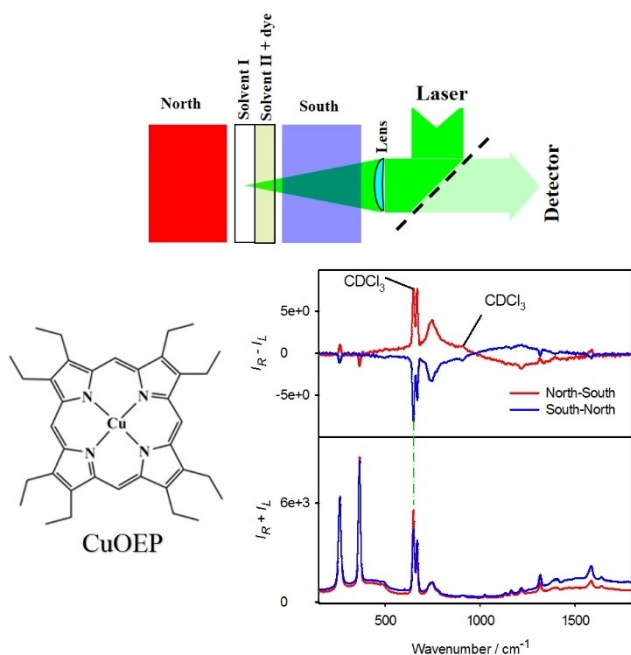


**Figure 1.** The magnetic ROA (MROA) experiment (top, schematically): The Cu(II) octaethylporphyrin complex (CuOEP, marked as “dye” and dissolved in  $\text{CHCl}_3$  (“solvent II”) is placed in a different cell than the same but deuterated solvent alone ( $\text{CDCl}_3$ , “solvent I”). Both of the cells are exposed to laser light and magnetic field. Raman ( $I_R + I_L$ ) and ROA ( $I_R - I_L$ ) spectra are plotted for two magnetic field orientations. Adapted from Ref. [11b] based on Creative Commons CC BY license.

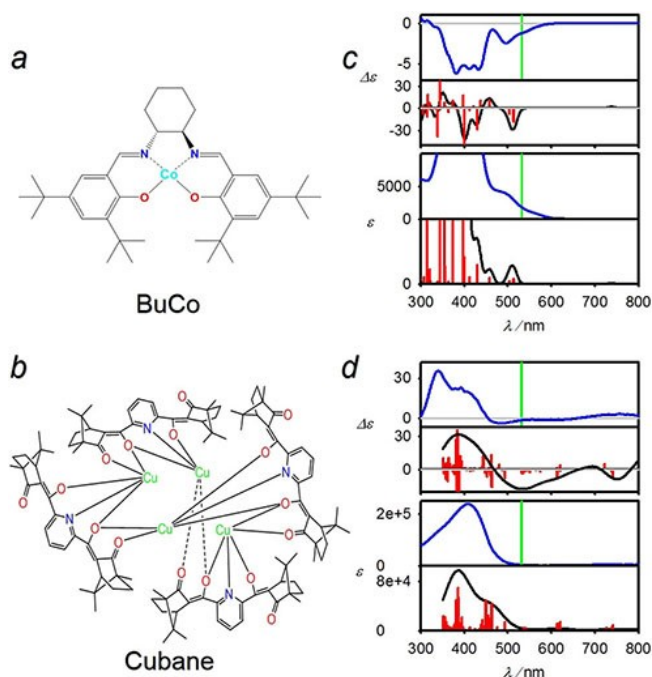


**Figure 2.** Chemical structural of two 3d metal coordination compounds and their electronic spectra. (a, b) (*R,R*)-(-)-*N,N'*-Bis(3,5-di-tert-butylsalicylidene)-1,2-cyclohexanediaminocobalt(II) (*R*-BuCo) and a tetrametallic copper(II) complex (*R*-Cubane, based on *R*-(+)-camphor). (c, d) corresponding absorption ( $\epsilon$ ) and ECD ( $\Delta\epsilon$ ) spectra, obtained by experiment (blue) and density functional theory (DFT) computation (black). 532 nm laser excitation is indicated by a green line, and individual computed transitions rendered in red. Reprinted with permission from Ref. [11a] (copyright 2022 American Chemical Society).

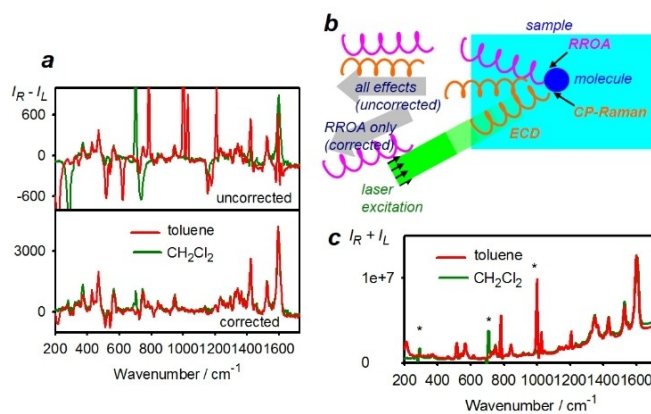


**Figure 3.** The extraction of molecular resonance ROA (RROA) signal of (*R,R*)-(-)-*N,N'*-Bis(3,5-di-tert-butylsalicylidene)-1,2-cyclohexanediaminocobalt(II) (*R*-BuCo) measured in two solvents (toluene and  $\text{CH}_2\text{Cl}_2$ ). (a) Raw spectra are ‘contaminated’ by the ECD-Raman contribution (top). Upon correction, pure RROA spectra are obtained (bottom). (b) The main events in the sample include (1) electronic circular dichroism (ECD) of the originally unpolarized laser light passing through the sample, (2) circular polarization changes due to Raman scattering on the molecule of interest (CP-Raman), (3) RROA of chiral molecules, and (4) ECD of the scattered light. All of these contribute to the total measured  $I_R - I_L$  circular polarization difference. (c) The corresponding Raman spectra of *R*-BuCo; asterisks (\*) indicate incomplete subtraction of the solvent Raman bands. Reprinted with permission from Ref. [11a] (copyright 2022 American Chemical Society).

thane ( $\text{CH}_2\text{Cl}_2$ ) as solvents. ECD of the solute is combined with Raman scattering, thus yielding ROA signals including vibrational bands of the solvent.<sup>[22]</sup> With the ECD-Raman subtraction formula, however, a more faithful RROA spectrum can be obtained, which is thus almost solvent-independent, as it should be.

To obtain RROA spectra, one has to measure the absorption and ECD spectra, such as the normal molar extinction coefficients at the wavelengths of incident- ( $e$ ,  $\Delta e$ ) and scattered-light ( $e'$ ,  $\Delta e'$ ). To minimize the path length not involved in scattering it is recommended to focus the laser in the sample close to the front cell window. In Ref.<sup>[11a]</sup> a more general formula, for the ECD-Raman contribution ( $I_{dif}^{\mu}$ ) to the recorded ROA intensity was used,

$$I_{dif}^{\mu} = \frac{1 - [1 + (e + e')c]e^{-(e+e')cl}}{2(e + e')(1 - e^{-(e+e')cl})} (I_{dif}^R \Delta e + I_{sum}^R \Delta e') \quad (2)$$

where  $c$  is the molar concentration of the complex,  $l$  is the Raman-active path length; and  $I_{sum}^R$  and  $I_{dif}^R$  are total and differential Raman intensities processed with right circularly polarized excitation light. Only under some conditions, this equation simplifies to Eq. 1.

The ECD-Raman contribution to ROA (Eq. 2) can be calculated for a broad range of absorption and ECD-Raman/RROA signal ratios, as described elsewhere.<sup>[20b]</sup> In Eq. 2, the intensity of ECD is assumed to be much weaker than absorption, which is generally true for most coordination compounds.

Encouraging results were obtained when the electronic transitions' contributions to Raman and ROA spectra of *R*-BuCo (Figure 2a) were simulated separately. Among the first 18

lowest-energy electronic transitions, only #8 yielded realistic Raman and ROA spectra. Close to the excitation wavelength (532 nm), this transition is associated with large electronic-transition dipole moment. When assigning the resonance states, one must take into account not only the spectral patterns, but also the signal's enhancement (absolute intensity). Some transitions (#8, #12, #15, and #16) involve a charge transfer across the ligands' aromatic system through the *d*-electron system in cobalt. These electronic transitions' localization also accounts for the rather selectively enhanced band at 1603  $\text{cm}^{-1}$  of the C=C aromatic bond stretching.

For a much bigger copper complex, Cubane (Figure 2b), the spectra calculated at pre-resonance conditions (532 nm) using molecular fragments reproduced the experiment reasonably well (Figure 4a) although the calculated C=O stretching signal ( $> 1590 \text{ cm}^{-1}$ ) was stronger than the measured one. A w-shape pattern (around 1535  $\text{cm}^{-1}$ ) almost dominated the RROA spectrum, mainly due to the C=C stretching within the ketone segment of the ligand scaffold, as validated by the simulation. There are approximately 190 fundamental vibrational transitions in the region of 1100–1450  $\text{cm}^{-1}$  were predominantly

associated with C–H bending. Additionally, some were linked to C–C stretching and other deformations. Notably, the pyridine breathing mode at 1044  $\text{cm}^{-1}$  yielded a rather strong Raman intensity, whereas the RROA signal within this range appeared relatively weak and most positive. Another w-shape RROA band appeared in the lower-frequency within 400–520  $\text{cm}^{-1}$ . It can be assigned to delocalized vibrations spanning the entire molecule, and computation reproduces it reasonably well.

In the “Cubane” complex, a greater number of electronic transitions are found close to the excitation wavelength (532 nm) than in “BuCo”. In the range of 490–550 nm, simulations predict 3 and 13 transitions for “BuCo” and “Cubane”, respectively. State #46 (transition wavelength estimated at 464 nm) seems to contribute most to Raman/RROA intensities; its Raman spectrum and RROA sign (negative) matches the experiment, and the overall resonance enhancement is extraordinarily high. Its transition charge density is shown in Figure 4b. Obviously, all double-bond electronic systems and copper *d*-electrons in all four ligands are involved, which likely translates to such a strong Raman signal.

A remarkable aspect of resonance Raman and ROA spectroscopy is demonstrated in Figure 4c. Raman intensities are due to the two types of camphor scaffolds; (I) camphors bridged to a copper atom through the carbonyl group, and (II) the other type. Under 2000 nm excitation, both of them contribute almost equally; this translates to their comparable chemical and optical properties. At 532 nm excitation, the carbonyl groups in the type II scaffold strongly contribute to the resonance and thus dominate the spectrum. In the type I residue, the carbonyl group that chelated to copper atom apparently reduces the involvement of  $\pi$ -electrons in electronic transitions featuring energies comparable to that of laser irradiation. Unlike for the main Raman and RROA bands around 1556  $\text{cm}^{-1}$ , the camphor scaffold is not manifested in the RROA spectra. Nevertheless, the residues can be recognized in the measured spectrum and correspond fairly well to the simulated data (Figure 4d).

The RROA spectroscopy of 3*d* metal coordination compounds appears to be suitable to discriminate between states with similar energies, and there is no other way to do that. It can provide information about delocalized electronic states spread over all the ligands, and metal *d*-electrons essential for the resonance effect contribute significantly to the spectra.

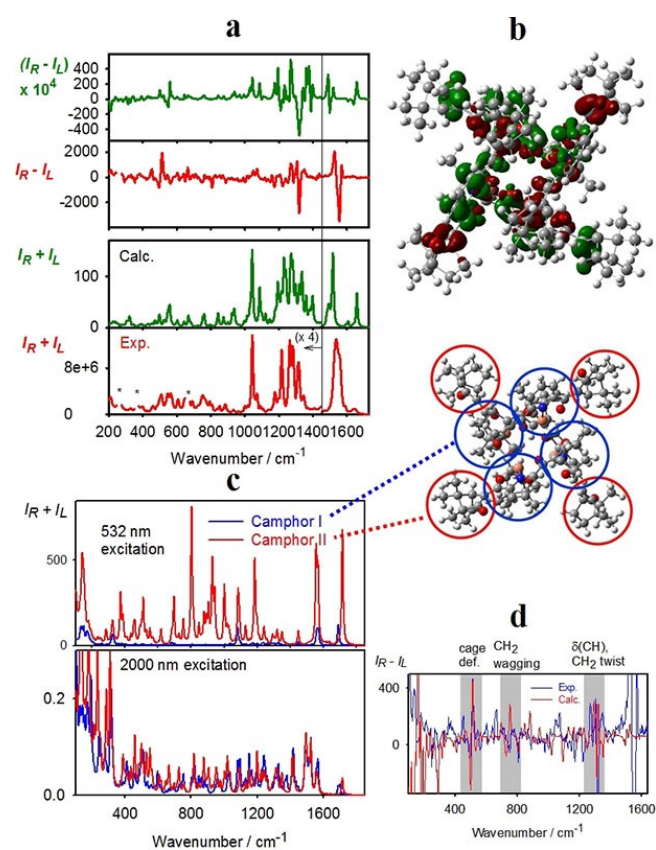


**Figure 4.** Raman and RROA spectra of *R*-Cubane. (a) Calculated (B3LYP/6-311++G\*\*/CCT/PCM) and experimental spectra. For the sake of clarity, the intensities were multiplied by a factor of 4 below 1450  $\text{cm}^{-1}$  (vertical separation line). (b) Transition charge density of an electronic transition #46, verified as main contributor to the resonance Raman (RROA) effect. (c) Calculated Raman spectra of the two types of camphor residues (I and II) at 532 and 2000 nm excitation. (d) Calculated RROA spectrum of the camphor residues only, and experiment data. Reprinted with permission from Ref. [11a] (copyright 2022 American Chemical Society).

### 3.4f Metal Coordination Compounds

The green (532 nm) light's energy is close to that of electronic transitions of some lanthanide(III) ions, e.g.  ${}^7F_0 \rightarrow {}^5D_1$  (520–530 nm) and  ${}^7F_1 \rightarrow {}^5D_1$  (530–540 nm) in the absorption spectra of Eu (III) compounds.<sup>[23]</sup> Molecules containing a europium (III) ion are thus expected to yield a stronger ROA signal, due to resonance. In addition, most lanthanide(III) ions also feature very specific sharp bands due to *f–f* luminescence; these are distributed across UV, visible, and near-infrared spectral areas.

The ROA spectrometer illuminates the sample by a laser, and the circularly polarized component is recorded by employing a highly sensitive, artifact-resistant detection scheme,<sup>[24]</sup>

even a very weak luminescence/fluorescence signal is thus detectable. As both Raman and luminescence bands are obtained simultaneously (i.e. in a single spectrum), their corresponding chiroptical counterparts may also be recorded simultaneously. Indeed, in the commonly used scattered circular polarization (SCP) ROA spectrometer, unpolarized laser illumination is employed, and the difference between the two circular polarizations is then detected at the emission side.<sup>[14]</sup> The CPL signal (if present) is thus mixed with the ROA signal. Likewise, if ROA is measured in the incident circular polarization (ICP) mode, fluorescence-detected circular dichroism (FDCCD)<sup>[25]</sup> signal may also be recorded jointly with the ROA signal.

Not surprisingly, earlier reports demonstrating that the europium (III) ion was capable of producing an intense and easily measurable signal in ROA spectra<sup>[26]</sup> attracted considerable attention. Indeed, the so-called "induced resonance ROA" was capable of detecting chirality in optically active ketones and alcohols upon their chelation to a non-chiral europium (III) complex.<sup>[27]</sup> The documented *CID* value of  $10^{-2}$  exceeded those found in numerous organic molecules and biomolecules,<sup>[14]</sup> and a similar result was obtained for a chiral bipyridine derived Eu(III) complex.<sup>[28]</sup> This made ROA spectra recording easier, and enabled use of reduced sample concentrations and/or shorter recording times.

Later, it was discerned that the robust chiral signals did not arise from Raman scattering or vibrational transitions. Rather, they emanated from a circular-polarization component of the luminescence exhibited by Eu(III) that was interacting with chiral substrate.<sup>[12c]</sup> For CPL measured on a ROA instrument (i.e., using a SCP-ROA detection scheme), the  $g_{lum}$  value can be easily converted to the *CID* value;  $g_{lum} = 2(I_L - I_R)/(I_L + I_R) = -2 \times CID$ .

The intense ROA signal observed in a chiral bipyridine-Eu(III) complex<sup>[28]</sup> was assumed to be mixed with the luminescence  $^5D_0 \rightarrow ^7F_1$  transitions of the Eu(III) ion. A hetero-metallic complex, cesium tetrakis(3-heptafluoro-butyryl-(-)-camphorato) Eu(III) ( $\Delta$ -CsEu[(-)-hfbc]<sub>4</sub>) and its enantiomer exhibit the highest CPL dissymmetry factor ever reported.<sup>[29]</sup> They were thus employed to assess the presence of circularly polarized luminescence in a ROA measurement. The Eu(III) transition  $^5D_0 \rightarrow ^7F_1$  band fits into the detector range of a commercial ROA instrument (~535–612 nm). As illustrated in Figure 5, distinct peaks are discernible in the vibrational Raman spectrum ( $I_R + I_L$ ) at 1989 and 1722  $cm^{-1}$ . Corresponding, robust ROA bands ( $I_R - I_L$ ) align with these peaks. Notably, the band at 1989  $cm^{-1}$  exhibits an extremely high *CID* value of 0.714 for the  $\Delta$  enantiomer, the largest value ever recorded in a ROA experiment. Furthermore, the value of  $2CID$  (1.43) measured on a ROA spectrometer is reasonably close to 1.38, this being the  $g_{lum}$  determined earlier by the CPL spectroscopy for the band at 595 nm.<sup>[29–30]</sup>

A useful quantity in the ROA spectroscopy is also the degree of circularity (*DOC*). It is defined for the left (*L*) and right (*R*) incident circularly polarized light as<sup>[31]</sup>

$$^R DOC = (I_R^R - I_L^R)/(I_R^R + I_L^R) \quad (3)$$

$$^L DOC = (I_R^L - I_L^L)/(I_R^L + I_L^L) \quad (4)$$

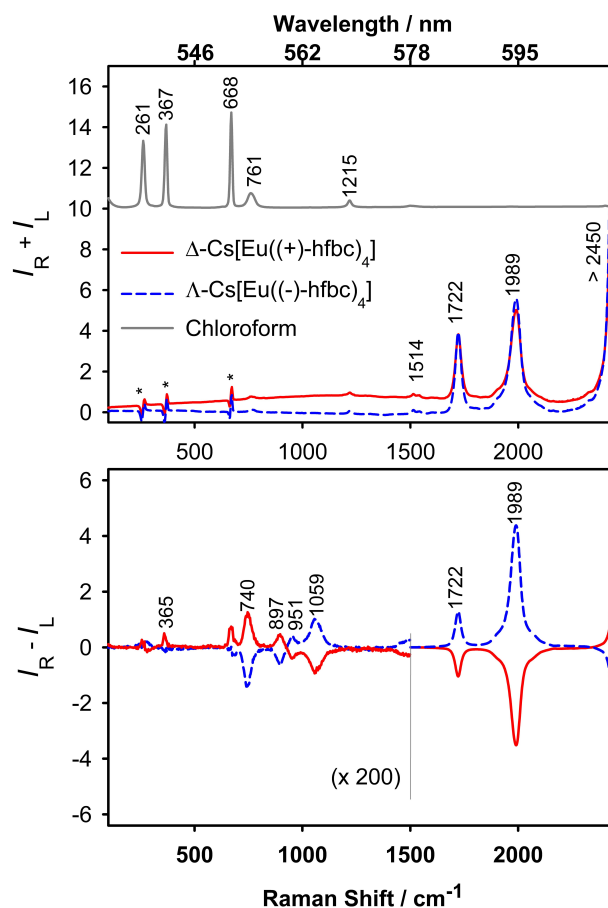


**Figure 5.** Raman (top) and Raman optical activity (ROA, bottom) spectra of two enantiomers of the Cs[Eu(hfbc)<sub>4</sub>] complex (2 mM in chloroform) acquired using 532 nm laser excitation. Raman spectrum of the solvent (chloroform) is shown in gray. ROA intensities below 1500  $cm^{-1}$  have been multiplied 200-fold to enhance visibility. Stronger Raman background in the  $\Delta$  enantiomer stems from fluorescent impurities. Slight artifacts (labelled by asterisks \*) emerge are due to incomplete subtraction of the chloroform signal. Adapted from Ref. [12c] (copyright 2015 John Wiley and Sons).

where the upper indices denote the *incident* polarization, i.e. the sign of *DOC* depends on it. As polarization is not preserved for the luminescence bands, the sign of the *DOC* signal from the Eu (III) complex remains unchanged as  $^R DOC = ^L DOC = CID$ . In this way, the ROA and CPL signals can be easily identified.

For achiral lanthanide compounds, luminophores can also be identified by optical activity induced by external magnetic field. The magnetic CPL (MCPL) spectra of the [Ln(DPA)<sub>3</sub>]<sup>3-</sup> complexes (Ln = Ce, Pr, Nd, Sm, Eu, Tb, Dy, Ho, or Er; DPA = dipicolic acid) were recorded on a ROA spectrometer during magnetic field exposure,<sup>[12b]</sup> and a wealth of luminescence bands of various lanthanide compounds could be obtained.

Out of the six weak lanthanide luminophores, namely Ce, Pr, Nd, Tb, Dy and Ho, their respective MCPL signal (Figure 6) is strongest in Tb(III) ( $^5D_4 \rightarrow ^7H_4$  and  $^5D_4 \rightarrow ^7H_5$  transitions)<sup>[32]</sup> and weakest in Ce(III) ( $^2D_{3/2} \rightarrow ^2F_{5/2}$  transition).<sup>[33]</sup>

Only Eu, Sm and Er yield luminescence spectra that are stronger (Eu) or at least comparable (Sm and Er) to the Raman spectra of a deprotonated DPA molecule. The luminescence

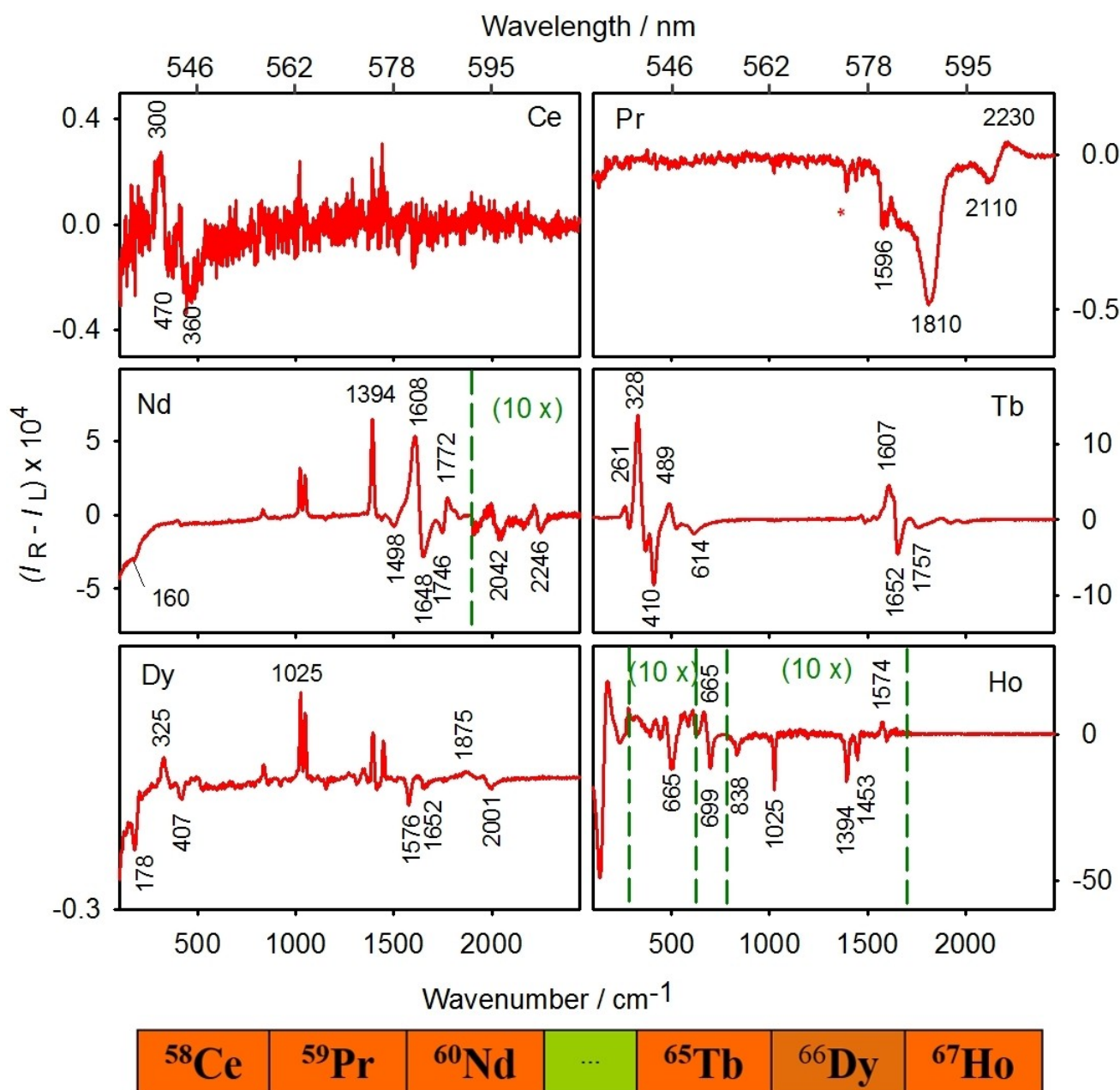


**Figure 6.** Magnetic circularly polarized luminescence (MCPL,  $I_R - I_L$ ) spectra of weakly-luminescent  $[\text{Ln}(\text{DPA})_3]^{3-}$  complexes in a magnetic field (1.5 T). Averaged spectra  $[S_{\text{ave}} = (S_{\text{North}} - S_{\text{South}})/2]$  normalized to maximum Raman intensity are shown. Adapted with permission from Ref. [12b] (copyright 2017 American Chemical Society).

bands of  $[\text{Sm}(\text{DPA})_3]^{3-}$  are predominantly governed by the  $^4G_{5/2} \rightarrow ^6H_{5/2}$  and  $^4G_{5/2} \rightarrow ^6H_{7/2}$  transitions in Sm(III). In the case of  $[\text{Eu}(\text{DPA})_3]^{3-}$ , the luminescence spectrum is mainly come from Eu(III)  $^5D_0 \rightarrow ^7F_1$  transition with bands at 1864 and 1976  $\text{cm}^{-1}$  accompanied by a large MCPL signal. On the other hand,  $[\text{Er}(\text{DPA})_3]^{3-}$  displays luminescence below 830  $\text{cm}^{-1}$ , comparable in intensity to the Raman signal of the DPA ligand prominent at higher wavenumbers. The  $^4S_{3/2} \rightarrow ^4I_{15/2}$  electronic transition is responsible for the most intense bands, as well as a MCPL “couplet” signal, exhibiting positive and negative bands at 328 and 362  $\text{cm}^{-1}$ .<sup>[12b]</sup>

Remarkably, magnetic ROA measurements disclose an intriguing correlation between MCPL and other spectroscopic modalities. In contrast to almost instantaneous Raman scattering (occurs within  $\sim$ fs), lanthanide luminescence proceeds at a slower pace (lifetime in the order of  $\mu$ s), so that the absorption and emission are well separated in time. In the context of SCP-ROA, the MCPL signal's polarization is affected by the energy levels of ground and excited electronic states of the emitted light. Typically, the lanthanide ion geometry changes encountered during the excitation are very small indeed, and the signal can thus be associated with the ground state's magnetic circular dichroism (MCD). For ROA experiment carried out with

incident circularly polarized light (i.e., employing the ICP-ROA detection scheme), MCPL is equivalent to magnetic FD-CD (FD-MCD), and the FD-MCD pattern can be related to absorption as all 4*f* states of the Ln (III) ions have almost identical geometries.

Lanthanide ions and their complexes strongly react to their environment. In particular, their achiral species can become optically active upon interaction with chiral molecules. Owing to this effect, the ROA-CPL detection scheme proved convenient to identify e.g. saccharides (Figure 7). Above 1500 cm<sup>-1</sup>, a strong CPL signal of the Eu(III)-sugar “complexes” was observed. As it is specific to the individual sugar species, it can be used to identify them.<sup>[34]</sup> Without the lanthanide complexes, it would be very difficult to distinguish the four monosaccharides from each other. Most prominently, EuCl<sub>3</sub> yielded very different spectra (red traces) for each of the four studied monosaccharides. Other applications of the ROA-CPL technique in biomolecular structural studies have been described in a recent review.<sup>[12a]</sup>

The above examples demonstrate the ROA instrument's versatility in lanthanide CPL measurements. This novel detection scheme has been designated as ROA-CPL. A significant benefit arises from the ability to directly excite the lanthanide ions using laser, with no need for a UV chromophore as an antenna ligand. The price paid for that is a limited spectral range of the detected luminescence as the transitions cannot be too far from the excitation wavelength (typically 532 nm). The range is about 535–612 nm in a currently available

commercial ROA instrument, but can be extended up to 700 nm in dedicated spectrometers.<sup>[35]</sup>

#### 4. Summary and Outlook

Electronic circular dichroism (ECD) and circularly polarized luminescence (CPL) are well established spectroscopic methods for stereo-chemical analysis of ground and excited states of chiral coordination compounds, and both of them also appear to be important in chiral Raman spectroscopy. The chirality can be generated in various ways, e.g. by introducing the Pfeiffer effect in a solution of racemate metal complexes using achiral ligands, by working with chiral ligands directly, or by employing chirality transfer in supramolecular structures.

The combination of ECD and resonance Raman optical activity (RROA) can provide unique information about electronic transitions in 3*d* metal coordination compounds. This is expected to be of use, for example, in structural studies of chromophores in bioinorganic chemical species such as metalloproteins essential for the functioning of living organisms.

The CPL measurement carried out using an inherently very sensitive ROA spectrometer tolerates reduced analyte concentrations and/or shorter acquisition times than in conventional ROA measurement. Induced CPL in lanthanide aids chiral

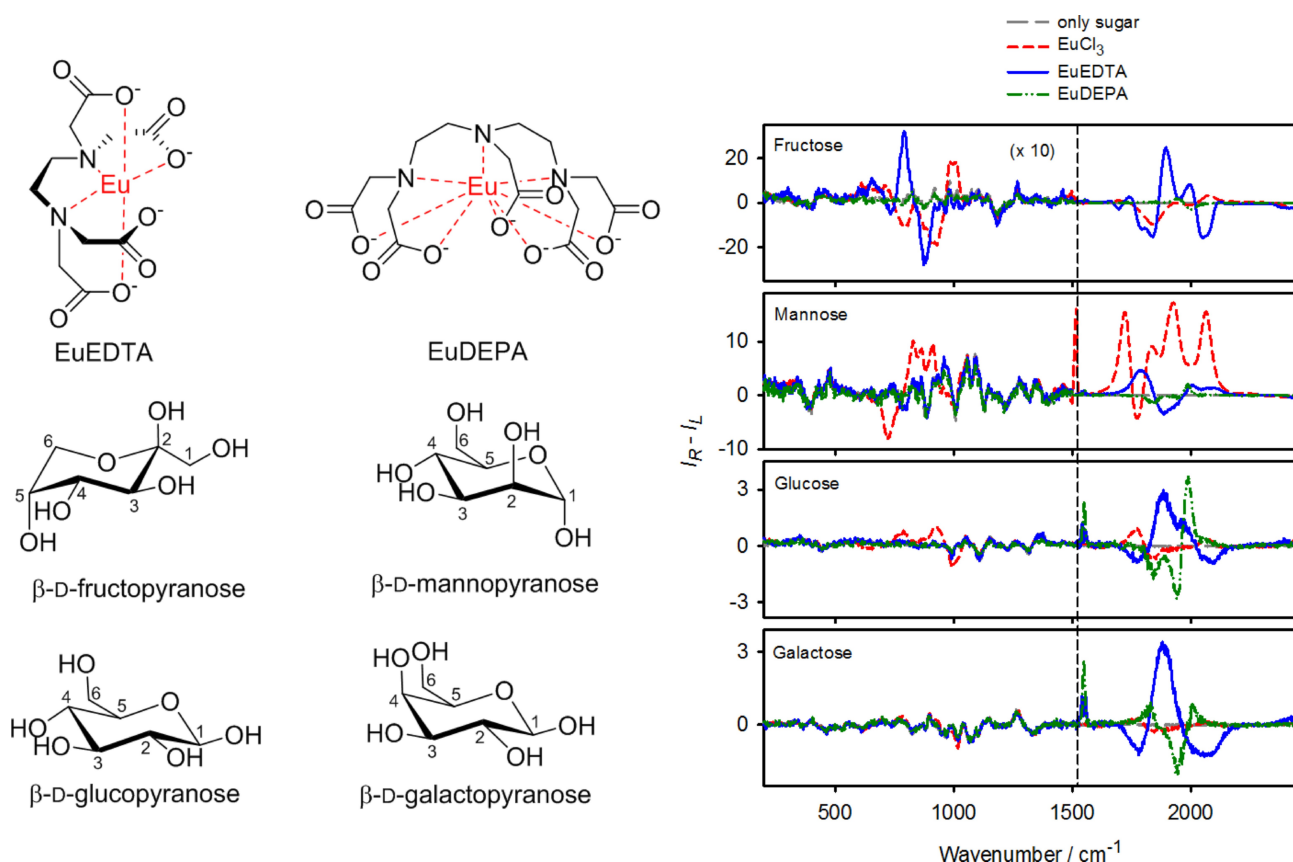


**Figure 7.** Raman optical activity (ROA,  $I_R - I_L$ ) spectra of four monosaccharides in the absence/presence of EuCl<sub>3</sub>, Na[EuEDTA] or Na<sub>2</sub>[EuDEPA]. Traces below ~1500 cm<sup>-1</sup> have been expanded ten-fold for the sake of clarity. Reprinted with permission from Ref. [34] (copyright 2016 American Chemical Society).

analyses of samples lacking conventional UV/vis chromophores, and structural studies of biomolecules such as saccharides.

The ECD-Raman and CPL components of the ROA signal can be significantly suppressed using longer excitation wavelengths. A ROA instrument equipped with a near-IR (785 nm) laser<sup>[36]</sup> makes it possible to directly record true vibrational Raman optical activity in most metal complexes. In this case, all advantages of the non-resonance ROA spectroscopy can be exploited although in this case, the signal is rather weak and acquisition times accordingly longer.

## Acknowledgements

The authors gratefully acknowledge support by the Czech Science Foundation (23-05378S to TW, 22-04669S to PB).

## Conflict of Interests

The authors declare no conflict of interest.

**Keywords:** circular dichroism · circularly polarized luminescence · coordination compounds · molecular chirality · Raman optical activity

- [1] a) J. M. Martín-Durán, B. C. Vellutini, A. Hejnov, *Phil. Trans. R. Soc. B* **2016**, 371, 20150411; b) Y. Shibazaki, M. Shimizu, R. Kuroda, *Curr. Biol.* **2004**, 14, 1462.
- [2] M. Schilthuizen, A. Davison, *Naturwissenschaften* **2005**, 92, 504.
- [3] G. Vantomme, J. Crassous, *Chirality* **2021**, 33, 597.
- [4] a) U. Knof, A. von Zelewsky, *Angew. Chem. Int. Ed.* **1999**, 38, 302; b) J. Crassous, *Chem. Soc. Rev.* **2009**, 38, 830; c) Z. Liu, W. He, Z. Guo, *Chem. Soc. Rev.* **2013**, 42, 1568; d) P. G. Lacroix, I. Malfant, C. Lepetit, *Coord. Chem. Rev.* **2016**, 308, 381; e) D. Parker, J. D. Fradgley, K.-L. Wong, *Chem. Soc. Rev.* **2021**, 50, 8193; f) W. Gong, Z. Chen, J. Dong, Y. Liu, Y. Cui, *Chem. Rev.* **2022**, 122, 9078; g) P. S. Steinlandt, L. Zhang, E. Meggers, *Chem. Rev.* **2023**, 123, 4764.
- [5] a) T. Wu, X. Z. You, P. Bouř, *Coord. Chem. Rev.* **2015**, 284, 1; b) P. L. Polavarapu, *Chiroptical Spectroscopy: Fundamentals and Applications*, CRC Press, Boca Raton, **2016**, p448; c) M. Krupová, J. Kessler, P. Bouř, *ChemPlusChem* **2020**, 85, 561; d) H. Sato, *Phys. Chem. Chem. Phys.* **2020**, 22, 7671–7679; e) S. C. J. Meskers, *ChemPhotoChem* **2022**, 6, e202100154; f) S. G. Telfer, T. M. McLean, M. R. Waterland, *Dalton Trans.* **2011**, 40, 3097.
- [6] a) L. A. Nafie, *Chirality* **2020**, 32, 667; b) L. D. Barron, A. D. Buckingham, *Chem. Phys. Lett.* **2010**, 492, 199-.
- [7] a) L. A. Nafie in *Chapter 14 - Vibrational Optical Activity: From Small Chiral Molecules to Protein Pharmaceuticals and Beyond*, (Ed. J. Laane), Elsevier, **2018**, pp. 421–469; b) T. A. Keiderling, *Chem. Rev.* **2020**, 120, 3381.
- [8] H. Sato, A. Yamagishi, *Int. J. Mol. Sci.* **2013**, 14, 964.
- [9] a) Y. Suffren, F.-G. Rollet, C. Reber, *Comment. Inorg. Chem.* **2011**, 32, 246; b) M. Wächtler, J. Guthmuller, L. González, B. Dietzek, *Coord. Chem. Rev.* **2012**, 256, 14798.
- [10] a) L. D. Barron, *Biomed. Spectrosc. Imaging* **2015**, 4, 223; b) S. Luber, *Biomed. Spectrosc. Imaging* **2015**, 4, 255.
- [11] a) T. Wu, J. Kapitán, P. Bouř, *J. Phys. Chem. Lett.* **2022**, 13, 3873; b) T. Wu, G. Li, J. Kapitán, J. Kessler, Y. Xu, P. Bouř, *Angew. Chem. Int. Ed.* **2020**, 59, 21895.
- [12] a) T. Wu, *Phys. Chem. Chem. Phys.* **2022**, 24, 15672; b) T. Wu, J. Kapitán, V. Andrushchenko, P. Bouř, *Anal. Chem.* **2017**, 89, 5043; c) T. Wu, J. Kapitán, V. Mašek, P. Bouř, *Angew. Chem. Int. Ed.* **2015**, 54, 14933.
- [13] R. J. H. Clark, T. J. Dines, *Angew. Chem. Int. Ed.* **1986**, 25, 131.
- [14] L. A. Nafie, *Vibrational Optical Activity: Principles and Applications*, J. Wiley & Sons, Chichester, U.K., **2011**, p 378.
- [15] L. D. Barron, *Molecular Light Scattering and Optical Activity*, Cambridge University Press, Cambridge, UK, **2004**, p 443.
- [16] a) M. Dudek, G. Zajac, A. Kaczor, M. Baranska, *J. Phys. Chem. B* **2016**, 120, 7807; b) G. Zajac, P. Bour, *J. Phys. Chem. B* **2022**, 126, 355; c) L. Nafie, *Vibrational optical activity: Principles and applications*, Wiley, Chichester, **2011**, p 378.
- [17] a) L. A. Nafie, *Chem. Phys.* **1996**, 205, 309; b) M. Vargek, T. B. Freedman, E. Lee, L. A. Nafie, *Chem. Phys. Lett.* **1998**, 287, 359.
- [18] a) S. Luber, J. Neugebauer, M. Reiher, *J. Chem. Phys.* **2010**, 132; b) C. Merten, H. G. Li, L. A. Nafie, *J. Phys. Chem. A* **2012**, 116, 7329.
- [19] M. Ziegler, A. von Zelewsky, *Coord. Chem. Rev.* **1998**, 177, 257.
- [20] a) G. Li, M. Alshalalfeh, W. Yang, J. R. Cheeseman, P. Bouř, Y. Xu, *Angew. Chem. Int. Ed.* **2021**, 60, 22004; b) E. Machalska, G. Zajac, A. J. Wierzbza, J. Kapitán, T. Andruniów, M. Spiegel, D. Gryko, P. Bouř, M. Baranska, *Angew. Chem. Int. Ed.* **2021**, 60, 21205.
- [21] a) J. Sebestik, F. Teply, I. Cisarova, J. Vavra, D. Koval, P. Bour, *Chem. Commun.* **2016**, 52, 6257; b) E. Machalska, G. Zajac, M. Baranska, D. Kaczorek, R. Kawęcki, P. F. J. Lipiński, J. E. Rode, J. C. Dobrowolski, *Chem. Sci.* **2021**, 12, 911; c) G. Li, J. Kessler, J. Cheramy, T. Wu, M. R. Poopari, P. Bouř, Y. Xu, *Angew. Chem. Int. Ed.* **2019**, 58, 16495.
- [22] G. Li, M. Alshalalfeh, J. Kapitán, P. Bouř, Y. Xu, *Chem. Eur. J.* **2022**, 28, e202104302.
- [23] K. Binnemans, *Coord. Chem. Rev.* **2015**, 295, 1.
- [24] W. Hug, *Appl. Spectrosc.* **2003**, 57, 1.
- [25] E. Castiglioni, S. Abbate, F. Lebon, G. Longhi, *Methods Appl. Fluoresc.* **2014**, 2, 024006.
- [26] C. Merten, H. G. Li, X. F. Lu, A. Hartwig, L. A. Nafie, *J. Raman Spectrosc.* **2010**, 41, 1563.
- [27] S. Yamamoto, P. Bouř, *Angew. Chem. Int. Ed.* **2012**, 51, 11058.
- [28] T. Wu, J. Hudcová, X. Z. You, M. Urbanová, P. Bouř, *Chem. Eur. J.* **2015**, 21, 5807.
- [29] J. L. Lunkley, D. Shirotani, K. Yamanari, S. Kaizaki, G. Muller, *J. Am. Chem. Soc.* **2008**, 130, 13814.
- [30] S. Di Pietro, L. Di Bari, *Inorg. Chem.* **2012**, 51, 12007.
- [31] W. Hug, G. Hangartner, *J. Raman Spectrosc.* **1999**, 30, 841.
- [32] J. C. G. Bunzli, *Chem. Rev.* **2010**, 110, 2729.
- [33] a) P. N. Hazin, J. W. Bruno, H. G. Brittain, *Organometallics* **1987**, 6, 913; b) Y. Liu, X. Wu, C. He, Y. Jiao, C. Y. Duan, *Chem. Commun.* **2009**, 45, 7554; c) P. N. Hazin, C. Lakshminarayan, L. S. Brinen, J. L. Knee, J. W. Bruno, W. E. Streib, K. Foltling, *Inorg. Chem.* **1988**, 27, 1393.
- [34] T. Wu, J. Průša, J. Kessler, D. Dračinský, J. Valenta, P. Bouř, *Anal. Chem.* **2016**, 88, 8878.
- [35] P. Michal, R. Čelechovský, M. Dudka, J. Kapitán, M. Vůjtek, M. Berešová, J. Šebestík, K. Thangavel, P. Bouř, *J. Phys. Chem. B* **2019**, 123, 2147.
- [36] a) L. A. Nafie, B. E. Brinson, X. L. Cao, D. A. Rice, O. M. Rahim, R. K. Dukor, N. J. Halas, *Appl. Spectrosc.* **2007**, 61, 1103; b) S. Haraguchi, M. Hara, T. Shingae, M. Kumauchi, W. D. Hoff, M. Unno, *Angew. Chem. Int. Ed.* **2015**, 54, 11555; c) J. Matsuo, T. Kikukawa, T. Fujisawa, W. D. Hoff, M. Unno, *J. Phys. Chem. Lett.* **2020**, 11, 8579.

Manuscript received: July 24, 2023

Revised manuscript received: August 31, 2023

Accepted manuscript online: September 4, 2023

Version of record online: ■■■, ■■■